This is a repository copy of *Effects of membrane curvature and pH on proton pumping activity of single cytochrome bo3 enzymes*.

White Rose Research Online URL for this paper:
https://eprints.whiterose.ac.uk/118162/

Version: Accepted Version

eprints@whiterose.ac.uk
https://eprints.whiterose.ac.uk/

Accepted Manuscript

Effects of membrane curvature and pH on proton pumping activity of single cytochrome bo_3 enzymes

Mengqiu Li, Sanobar Khan, Honglin Rong, Roman Tuma, Nikos S. Hatzakis, Lars J.C. Jeuken

Please cite this article as: Mengqiu Li, Sanobar Khan, Honglin Rong, Roman Tuma, Nikos S. Hatzakis, Lars J.C. Jeuken, Effects of membrane curvature and pH on proton pumping activity of single cytochrome bo_3 enzymes, *BBA - Bioenergetics* (2017), doi:10.1016/j.bbabio.2017.06.003

Effects of membrane curvature and pH on proton pumping activity of single cytochrome bo_3 enzymes

Mengqiu Li[1], Sanobar Khan[2], Honglin Rong[1], Roman Tuma[3], Nikos S. Hatzakis[4,*], Lars J. C. Jeuken[1,*]

[1] School of Biomedical Sciences, University of Leeds, LS2 9JT Leeds, U.K.
[2] School of Chemistry, University of Leeds, LS2 9JT, Leeds, UK
[3] School of Molecular and Cellular Biology, University of Leeds, LS2 9JT, Leeds, U.K.
[4] Nano-Science Center, Department of Chemistry, University of Copenhagen, Copenhagen 2100, Denmark

[*]Corresponding author:
Nikos S. Hatzakis, Hatzakis@nano.ku.dk
Lars J.C. Jeuken, L.J.C.Jeuken@leeds.ac.uk

ABSTRACT

The molecular mechanism of proton pumping by heme-copper oxidases (HCO) has intrigued the scientific community since it was first proposed. We have recently reported a novel technology that enables the continuous characterisation of proton transport activity of a HCO and ubiquinol oxidase from *Escherichia coli*, cytochrome bo_3, for hundreds of seconds on the single enzyme level (Li *et al* J Am Chem Soc 137 (2015) 16055-16063). Here, we have extended these studies by additional experiments and analyses of the proton transfer rate as a function of proteoliposome size and pH at the *N*- and *P*-side of single HCOs. Proton transport activity of cytochrome bo_3 was found to decrease with increased curvature of the membrane. Furthermore, proton uptake at the *N*-side (proton entrance) was insensitive to pH between pH 6.4-8.4, while proton release at the *P*-side had an optimum pH of ~7.4, suggesting that the pH optimum is related to proton release from the proton exit site. Our previous single-enzyme experiments identified rare, long-lived conformation states of cytochrome bo_3 where protons leak back under turn-over conditions. Here, we analyzed and found that ~23% of cytochrome bo_3 proteoliposomes show ΔpH half-lives below 50 s after stopping turnover, while only ~5% of the proteoliposomes containing a non-pumping mutant, E286C cytochrome bo_3 exhibit such fast decays. These single-enzyme results confirm our model in which HCO exhibit heterogeneous pumping rates and can adopt rare leak states in which protons are able to rapidly flow back.

1

Introduction

Cytochrome bo_3 is an ubiquinol oxidase and a terminal oxidase in *Escherichia coli*. As a member of the A-type heme-copper oxidase (HCO) family, cytochrome bo_3 is homologous to the mitochondrial Complex IV/cytochrome *c* oxidase [1, 2] and binds oxygen at its heme-copper bi-nuclear center (BNC) where the oxygen molecule is reduced to water [3]. A marked distinction between the two protein complexes is that cytochrome *c* oxidase receives electrons from a single-electron donor, cytochrome *c*, whereas cytochrome *bo₃* has a two-electron donor, ubiquinol. Oxygen reduction is coupled to the movement of protons, resulting in the uptake and release of protons involved in two different processes: 1) protons participating in the redox reactions ("chemical protons") and 2) protons transported across the membrane ("pumped protons") [1, 4-8]. During normal turnover, "chemical protons" and "pumped protons" both contribute to the transmembrane electrochemical gradient ($\Delta\psi$) and pH gradient (ΔpH), which together constitute the proton motive force (*pmf*), the driving force for the synthesis of adenosine triphosphate (ATP) [1]. The chemical and pumped protons together account for eight protons transferred across the membrane per oxygen molecule reduced, giving a stoichiometry of 2 H^+/e^- [3].

The molecular mechanism of proton pumping by HCOs has intrigued the scientific community since it was first proposed [1, 4-18]. It is generally accepted that proton pumping is achieved by coupling electron transfer steps or redox states of BNC to the orchestrated protonation of key amino acid residues and/or water molecules [8, 17, 18]. Two proton entry pathways have been identified for HCOs and are named after amino acids that are considered to play important roles in each channel. These are the D- and K-channels, where the D-channel takes up both chemical and pumped protons and the K-channel only takes up chemical protons. At the end of the D-channel, a crucial glutamate is located (E286 for *E. coli* cytochrome bo_3), which is believed to act as a gate, preventing backflow of protons during turn-over [6]. The proton exit pathway is less clearly defined, although a key proton-loading site (PLS) has been identified at one of the propionate group of the heme that is part of the BNC [19].

The protonation state of residues at the entrances and exits of the proton channels in HCOs are affected by the pH on each side of the membrane, and thus pH is expected to affect the proton pumping and redox activities of the enzymes. The effect of pH on the oxygen reduction activity was found to be different for the two sides of *Rhodobacter sphaeroides* cytochrome *c* oxidase. In particular, the enzyme activity was observed to change with the pH

2

at the *N*-side (proton entrance) of the enzyme, but remained relatively unaltered upon changing the pH at the *P*-side (proton exit) [20].

We have recently published a novel methodology in which the proton transport activities of single cytochrome *bo*$_3$ enzymes are continuously monitored for hundreds of seconds [16]. In this method, which is schematically shown in Fig. 1, proteoliposomes are prepared with a low protein-to-lipid ratio, such that only 1 in ~10 liposomes contains a (single) cytochrome *bo*$_3$. The (proteo)liposomes are sparsely adsorbed on transparent, gold coated, microscopy slides so that individual vesicles can be optically monitored. The pH in the lumen of the (proteo)liposomes is monitored via a membrane impermeable pH-dependent fluorescent dye, which are encapsulated in the vesicles. After a set period of time, typically 100s, the ubiquinone pools in the (proteo)liposomes are electrochemically reduced, which initiates and sustains proton transportation by cytochrome *bo*$_3$ in proteoliposomes. The electrical potential is switched off again after a set period of time, usually 100s, and the enzymes enter their rest state as the ubiquinol pool in the vesicles is exhausted within the temporal resolution of the experiment [16]. Fluorescence images are taken continuously throughout the three stages of the experiments: the pre-potential period (enzyme at rest), potential window (enzyme active), and post-active period (enzyme at rest). The experiments were carried out on the wild-type (WT) cytochrome *bo*$_3$ in the absence and presence of valinomycin, which abolishes Δψ, and on E286C cytochrome *bo*$_3$ in which the glutamate "gate" has been mutated. This mutant still reduces oxygen to oxidize ubiquinol, transporting "chemical protons" across the membrane in the process, but is unable to "pump" protons [21].
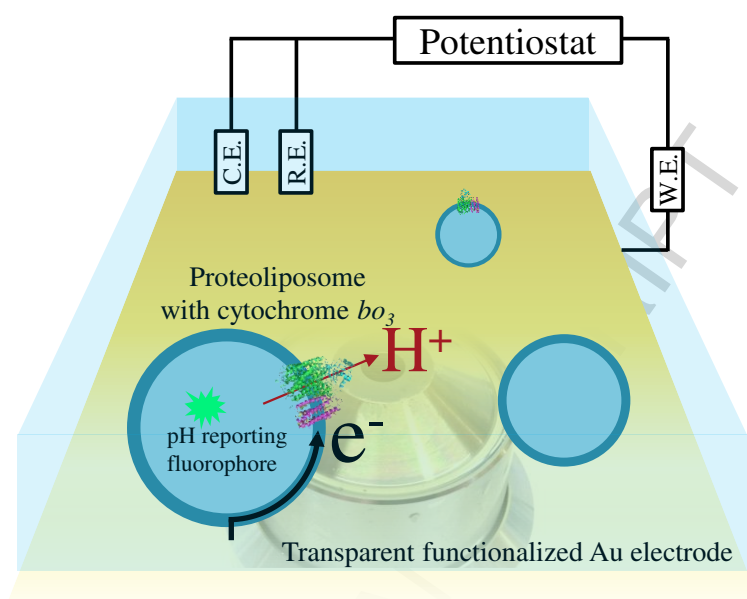
Fig. 1. Schematic representation of the experimental method. A custom-built electrochemical cell enables the continuous monitoring of the fluorescence signal with an inverted microscope. Proteoliposomes with a low protein-to-lipid ratio are sparsely adsorbed on a transparent gold coated slide, which acts as an electrode in a 3-electrode system: working electrode/gold electrode (W.E.), counter electrode (C.E.), and reference electrode (R.E.). While fluorescent images are recorded, a potential of -0.2V vs. standard hydrogen electrode (SHE) is applied to the W.E. to reduce the ubiquinol pool within the liposomes, which initiates and sustains the proton transport by the reconstituted cytochrome bo_3 complexes. The pH change in the lumen of the proteoliposomes, as the result of the enzyme activity, is monitored by recording the fluorescence signal of a membrane impermeable, pH-sensitive dye that is encapsulated in the (proteo)liposomes.

Single-enzyme measurements have the key ability to detect rare conformational states and the single-enzyme experiments on cytochrome bo_3 identified the previously unknown long-lived "stalled" and "leak" states [16]. In the stalled state, cytochrome bo_3 stops transporting protons in spite of the supply of ubiquinol and oxygen. More surprising was the observation of leak states during which protons rapidly and freely flowed backwards, dissipating the transmembrane energy gradients [16]. In our previous work, we showed that the relative frequency of the enzyme entering either the stalled or the leak state is correlated to the ΔpH [16]. Using a similar methodology, similar stalled and leak states were also observed in single-enzyme studies of the prototypic proton-pumping P-type ATPase from *Arabidopsis thaliana* isoform 2 (AHA2) [22]. In the present study, we have extended our single-enzyme analysis of cytochrome bo_3 and show that (a) increased membrane curvature reduces proton pumping activity; (b) leak states might be retained by cytochrome bo_3 directly after turn-over has been halted and; (c) proton transport activity is mostly affected by the pH on the *P*-side.

Results and Discussion

Fig. 2 shows examples of the time traces of individual proteoliposomes and liposomes. The two vertical dotted lines indicate the time period during which the potential is switched on and off again. A potential of –0.2 V vs Standard Hydrogen Electrode (SHE) is applied as we have previously shown that reducing the potential below -0.2V does not further enhance the activity and hence the ubiquinone-10 reduction is no longer rate limiting [23]. Cytochrome bo_3 is thus active in between the dotted lines. The pH change in the lumen of the (proteo)liposomes has been converted to the number of transported protons, taking into account the size of the individual proteoliposomes and buffering capacity of individual components in the system (see Material and Methods for details). Positive number of transported protons corresponds to protons being translocated out of the vesicle (from the lumen to the bulk solution), and *vice versa*. The presence of proton transport in both directions reflect the random orientation of the complex. The majority (~85%) of the time traces are flat and featureless (Fig. 2 bottom right) because at this low protein-to-lipid ratio most of the vesicles do not contain a cytochrome bo_3 complex. Of the proteoliposomes that show active proton translocation, the majority (>80%) show a constant steady-state activity, demonstrated by linear increase or decrease in the number of transported protons while the potential is applied (Fig. 2, top).
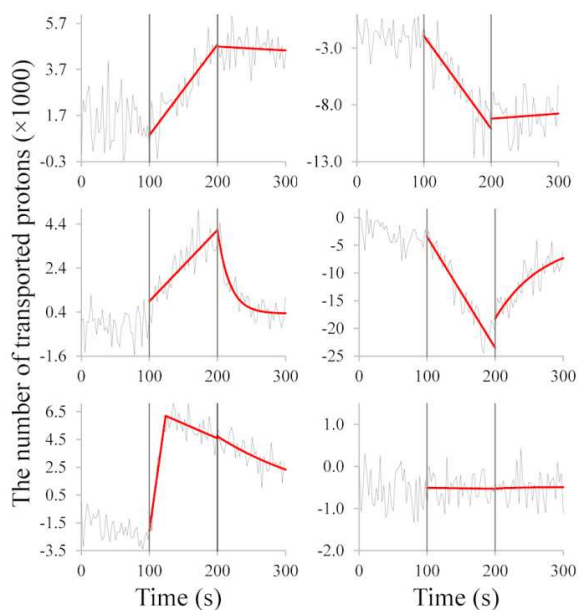
Fig. 2. Examples of time traces of individual proteoliposomes/liposomes. Positive number of transported protons corresponds to outwards proton translocation (from intravesicular space to the bulk solution), and *vice versa*. Example traces are given for proteoliposomes where protons are pumped throughout the application of the electrical potential without observable proton leakage (top left & top right), proton leakage observed in the post-active period (middle left & middle right), and proton leakage observed within the electrical potential window which appears to continue into the post-active period (bottom left). An example of liposome without cytochrome *bo₃* is also shown (bottom right). Solid red lines are fits to the data (solid gray) as explained in the text. Proton uptake/release activity was initiated by applying an electrical potential between 100s and 200s as indicated by the vertical dashed lines.

Effects of membrane curvature

Membrane curvature affects the activity of many membrane proteins, and some membrane proteins have been shown to change membrane curvature [24-26]. In Fig 3, the proton translocation activity of cytochrome bo_3 is thus analyzed in relation to proteoliposomes size, which indicates that the proton transport rate is indeed correlated to the membrane curvature. We note that to compile Fig. 3, only data has been used where cytochrome bo_3 actively transport protons, i.e., stalled and leak states have been omitted. As explained in the introduction, pH changes in the lumen are measured via an encapsulated fluorescent dye. The size of proteoliposomes were determined independently, by doping the lipid vesicles with fluorescent lipid analogues and using the intensity of this fluorescence to determine the size, which is calibrated using dynamic light scattering [27]. As shown in the top of Fig. 3 (white bars), the rate of pH change is largely constant with proteoliposome size. However, the volume of the internal lumen and the number of phospholipids in a vesicle are dependent on its size and both properties affect the buffer capacity of the vesicle. As a result, smaller vesicles should display larger pH changes when a fixed number of protons is transported. Indeed, when the rates of pH changes (which are size independent) are converted to the rates of proton transportation (see Materials and Methods for details), cytochrome bo_3's activity is shown to be strongly dependent on the proteoliposome size, i.e., the enzyme is more active in low-curvature membranes (Fig. 3, bottom). This is in agreement with earlier studies that suggest that the structure and function of transmembrane proteins can be influence by membrane curvature [28-31].

In the single enzyme proteoliposomes, cytochrome bo_3 is found in both orientations, either transporting protons into or out of the lumen. The effect of membrane curvature was also determined for either orientation separately, but no significant differences were observed between both orientations (not shown) and hence, in Fig. 3, transport by cytochrome bo_3 in both orientations is combined. Cytochrome bo_3 has a large degree of asymmetry with the ubiquinol active site and proton entry and exit sites on different sides of the membrane. The absence of any effect on protein orientation is thus perhaps unexpected, but consistent with a model in which higher membrane tensions induce general allosteric effects on enzymes as a whole (rather than in orientation dependent manner) [28-31].

The effect of membrane curvature is sufficiently large that it should be observable in ensemble experiments. To test this, an ensemble experiment was performed in which the decylubiquinol (DQ) oxidation activity of cytochrome bo_3 was determined in proteoliposomes of different sizes. Proteoliposomes were prepared identically to the single-

enzyme experiments, but with a higher protein-to-lipid ratio. Ten freeze-thaw cycles were performed to increase size of the proteoliposomes to a diameter of 518 ± 23 nm, which was determined by dynamic light scattering (the polydispersity index, PDI was approx. 0.52). The DQ oxidation activity was found to be 39 ± 3 DQ/s (at a DQ concentration of 34 µM). The same proteoliposome preparations were then extruded to reduce the size of the vesicles to 95 ± 1 nm (PDI was approx. 0.06) and the activity was measured again under identical condition to be 21 ± 2 DQ/s, approximately half of that observed for the larger vesicles. Although the ensemble experiments show less effect of curvature than the single-enzyme experiments, they still confirm the general correlation between activity and vesicle size. The fact that the ensemble experiments show less effect of curvature might be due to a number of reasons, including the higher PDI of the larger vesicles, which indicates a mixture of vesicle sizes for this preparation.

The transport of protons into or out of the proteoliposomes contributes to both ΔpH and $\Delta\psi$, but only the former is determined in our experiments. At sufficiently high *pmf*, the activity of cytochrome bo_3 is expected to decrease, but without quantifying $\Delta\psi$ this cannot be experimentally confirmed. To study the effect of $\Delta\psi$ in the single enzyme experiments, $\Delta\psi$ was abolished by the addition of valinomycin in a potassium buffer (Fig. 3). Two opposing effects were observed. First, adding valinomycin resulted in the anticipated increase in proton transporting activity, but only for vesicles smaller than ~140 nm. This effect, which is more clearly seen in the rate of pH change (Fig. 3, top), appears to be eliminated for larger vesicles, such that proton transport activity slightly decreased. We propose that in the smaller vesicles, proton transport creates a significant $\Delta\psi$, which together with ΔpH, limits the activity of cytochrome bo_3. When $\Delta\psi$ is abolished by the addition of valinomycin [32], the average proton transport rate increases. In contrast, in the larger vesicles, the build-up of $\Delta\psi$ by a single enzyme might be less pronounced and a previously observed, direct inhibitory effect of valinomycin [33] might offset the effect of dissipating $\Delta\psi$. The increased error bars in proton transport for larger diameters (Fig. 3, bottom) make it hard to record the anticipated plateau for larger vesicles.

8

☐WT *bo*$_3$ without valinomycin
☐WT *bo*$_3$ with valinomycin
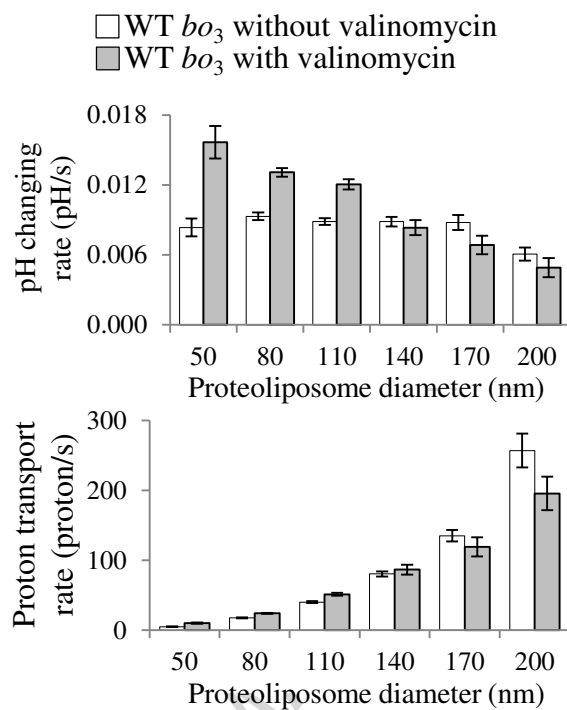
Fig. 3. The effect of the size of proteoliposomes on the activity of cytochrome *bo*$_3$. The top panel corresponds to the pH changing rate, while the bottom panel corresponds to rate of proton transportation (calculated from the pH changing rate and the independently measured proteoliposome diameter). Error bars represent the standard error of the mean. Negative rates (inwards proton transportation) have been converted to absolute values.

Proton leakage in the post-active state

An example of a long-lifetime proton leak state that is occupied by cytochrome bo_3 under turn-over conditions is shown in Fig. 2, bottom left. We have presented a detailed analysis of these rare leak states under turn-over conditions previously and they were observed in 7.2% of the proteoliposomes [16]. Here we extended this analysis by testing whether proton leakage continues when the electrochemical potential is switched off and, consequently, the ubiquinol substrate is depleted. Hereafter, cytochrome bo_3 during this period will be referred to as in the "post-active state".

As described in the method section, the time traces during the post-active state were fitted with a single-exponential curve (see also Fig. 2), where the half-life of the proton leakage is derived from the fitted parameters. A significant proportion of the proteoliposomes with cytochrome bo_3 shows significant leakage in the post-active phase and more than half the proteoliposomes show half-lives below 500 s (Fig. 4, top, white bars). However, liposomes are known to exhibit an intrinsic "background" permeability towards protons [34]. To test whether cytochrome bo_3 contributes to the observed leakage in the post-active phase or whether the leakage is due to background permeability, the same analysis was performed with a mutant of cytochrome bo_3, E286C. Fig. 4 (top, grey bars) shows that E286C cytochrome bo_3 displays significantly fewer leakage events with a half-live below 100 s.

We have previously performed pH jump experiments in which proteoliposomes with WT or E286C cytochrome bo_3 were subjected to a sudden pH change of ~0.5 units (Supplementary information of reference [16]). These proteoliposomes were prepared with a higher protein-to-lipid ratio to ensure each liposome contained cytochrome bo_3. Here, we have re-analyzed these pH jump experiments to determine half-lives of the pH gradients (Fig. 4, bottom). It is clear that in these pH jump experiments, liposomes of this study with WT (or E286C) cytochrome bo_3 do not exhibit significant proton leakage with half-lives below 100 s. In contrast, slower leakages with half-lives above 100 s are observed, which we ascribe to background permeability of the liposomes.

Together, these observations show that in the "post-active state", a significant fraction of proteoliposomes with WT cytochrome bo_3 exhibit fast proton leakage (half-lives < 100 s) that is not due proton permeability of the proteoliposomes (i.e., background leakage). This strongly suggest that proton leakage with half-lives below 100 s occurs through the enzyme. It is unclear to what extend this leakage is identical to the leak state we previously identified in proteoliposomes with WT cytochrome bo_3 under turn-over conditions. Importantly, leakage with half-lives below 100 s is not observed in pH jump experiment where

10

cytochrome bo_3 has not been active, consistent with the idea that cytochrome bo_3 at "rest" (oxidized **O**-state) does not leak protons. We note that the post-active leakage is observed either as a continuation of the leakage initiated during conditions that support turn-over (Fig. 2, bottom left) or immediately when commencing the post-active period (Fig. 2, middle). Presumably, in the former, the leak state simply continues when the electrochemical potential is switched off at the start of the "post-active" phase.

We note that we have previously confirmed that leakage is reversible, i.e., proteoliposomes that display leakage return to a non-leaking state (Figure S3 of the Supplementary Information in [16]). We observed that the percentage of (proteo)liposomes in consecutive time-trace experiments on a single electrode is constant. Would leaking proteoliposomes not be able to return to a non-leak state, this percentage would have decreased. Furthermore, we previously also determined that addition of valinomycin did not change the frequency by which leak states were observed[16]. This suggests that the probability by which cytochrome bo_3 can adopt a leak state is not dependent on $\Delta\psi$. We note, however, that valinomycin did affect the leak rate, suggesting that $\Delta\psi$ contributed to the kinetics by which protons flow back once a leak state is adopted by cytochrome bo_3.

Previously, the group of Verkhovsky showed that proteoliposomes containing cytochrome c oxidase from either bovine or *Paracoccus denitrificans* exhibit faster relaxation of the $\Delta\psi$ when the enzyme is in the O_H state (the O_H state is the fully oxidized form of HCO that is formed when a fully reduced enzyme reacts with oxygen) [35]. Relaxation times, τ, below 0.5 - 0.8 s were observed for the O_H state compared to much slower relaxation ($\tau > 3$ s) for the reduced cytochrome c oxidase. Interestingly, the fast relaxation behavior was absent in a mutant in which the D-channel was blocked (D124N cytochrome c oxidase), which led to the conclusion that the fast relaxation was due to proton conductance through the D-channel in the O_H state and that cytochrome c oxidase could leak by uncoupling or slipping between electron and proton transport. The $\Delta\psi$ relaxation times (τ) are much faster than reported here for ΔpH, but the experimental systems are not directly comparable. The dissipation of $\Delta\psi$ was measured in an ensemble experiment after a photo-induced single turn-over, where the second turn-over was limited by the presence of CO. In spite of the fact that the two experimental systems greatly vary, we are wondering whether also the post-active leak states could be explained by different oxidation states of cytochrome bo_3. By abruptly halting the electrochemical ubiquinol oxidation, a heterogeneous population of cytochrome bo_3 enzymes

11

could arise with different oxidation states, some of which may correspond to the leaky O_H state.

In this respect we note a very recent publication by the group of Brzezinski, in which single-enzyme experiments were performed with cytochrome bo_3, but under their experimental conditions no leak state was observed during continuous turn-over [36]. This is in contrast to our experiments, the analysis by Verkhovsky discussed in the previous paragraph[35] as well as leak states observed with another structurally unrelated enzyme, P-type ATPase [22]. A detailed discussion of the differences in methodology between the two studies and how they could be responsible for the observed difference falls outside the scope of this paper. However, it would be interesting to examine whether there is an effect of the different substrate homologues used in both studies (ubiquinol-1 versus the lipophilic ubiquinol-10) and its potential correlation to oxidative and leaking states of cytochrome bo_3 or whether the temporal resolution affects the observations. The fact, however, that we and others have observed leaking in multiple structurally unrelated proton transporters suggests that leaking could be a general feature reflecting stochastic nature of transporter function at single molecule level.

Finally, one might question to what extend the leak states contribute to the maximum ΔpH that can be generated by cytochrome bo_3. The maximum ΔpH observed in our experiments is 2 units, although very few liposomes are observed with a ΔpH > 1.5. 2 pH units is equivalent to an electrochemical potential of ~120 mV, close to the value reported for the plasma membrane in *E. coli* cells [37]. We have previously shown that the probability of the leak and stalled states increases at higher ΔpH [16]. Thus, it is possible that when ΔpH reaches saturating conditions, the enzyme simply stops or stochastically starts leaking. However, due to the low number of liposomes that are obtained at ΔpH > 1.5, it is hard to make statistically robust conclusions on whether and, if so, how the leak states limit the maximum attainable ΔpH.

☐ WT cytochrome bo_3
☐ E286C cytochrome bo_3

Post-active proton leakage

%

Proton leaking half-life (s)

☐ WT cytochrome bo_3
☐ E286C cytochrome bo_3

pH-jump proton leakage

%

Proton leaking half-life (s)
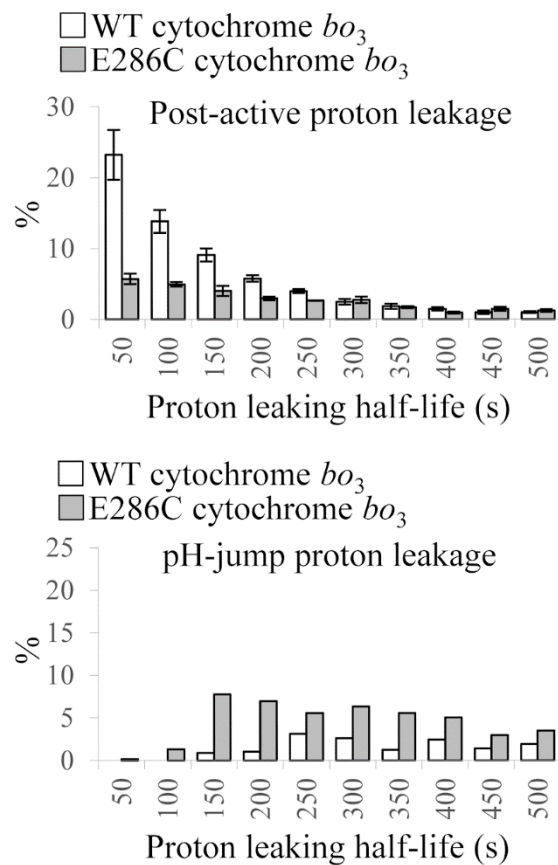
Fig. 4 The distribution of the proton leakage half-life of proteoliposomes after the electrical potential was switched off (Top, enzyme inactive) and after a pH jump of 0.5 units was applied (Bottom). The white and grey colors correspond to WT and E286C cytochrome bo_3, respectively. Only half-life values below 500 s are shown as higher values cannot confidently be determined in the 100 s time period the post-active state was monitored.

pH effects on proton transport activity

As discussed in the introduction, the pH on the *N*-side of the closely related cytochrome *c* oxidase has been shown to be fully accountable for the overall pH-dependency on the O_2 reduction activity and kinetics of proton uptake and electron transfer in the pH-interval 6–9.5 [20]. The aforementioned study was performed at the ensemble level and the pH in the lumen and extravesicular ("bulk") buffer were set so that the enzymes did not work against a ΔpH. In contrast, the present study investigates cytochrome *bo*₃ on the single-enzyme level. Here, when cytochrome *bo*₃ is activated and starts transporting protons, the lumen pH increases or decreases depending on the random orientation of the protein complex in the proteoliposome (Fig. 2). The extravesicular pH remains constant at 7.4 because the volume of the lumen of proteoliposomes absorbed in the surface is negligible compared to the relatively large volume of buffered solution.

If the intravesicular pH is the same as the outside, the enzymes build a ΔpH against the proton transportation as soon as they become active. Importantly, however, before activating cytochrome *bo*₃ (the pre-potential period), the pH in the lumen was observed to vary between single proteoliposomes with a distribution around the bulk pH 7.4. Thus, the distribution of the lumen pH at the start of the time traces enables us to monitor enzymes transporting proton along, as well as against, ΔpH, while at the same time monitor the effect of absolute pH values. As both orientations of the enzymes in the proteoliposomes are present, the present study contains data for 4 types of condition for proton transportation: outwards against ΔpH (Fig. 5, left, shaded bars), outwards along ΔpH (Fig.5, left, clear bars), inwards against ΔpH (Fig. 5, right, shaded bars), and inwards along ΔpH (Fig. 5, right, clear bars). Fig. 5 (top) shows that the pH-dependency of WT cytochrome *bo*₃ is different on the two sides of the enzyme: proton uptake at the *N*-side (proton entrance, Fig. 5, left) is insensitive to pH between pH 6.4-8.4 (the seemingly higher rates at lower pH are not statistically relevant); in contrast, proton release at the *P*-side (proton exit, Fig. 5, right) has an optimum pH of about 7.4. The same experiment was repeated in the presence of valinomycin to negate any potential contribution of Δψ (Fig. 5, middle). A similar pH dependency is observed with valinomycin, although there is now a possible pH effect apparent at the *N*-side, but with a much smaller magnitude as that of the *P*-side.

Cytochrome *bo*₃ has two proton channels conserved in the Type-A heme-copper oxidases, known as the K- and D-channel, both of which lead to the heme-copper BNC where oxygen is reduced [1, 4, 9, 38]. The K-channel transports protons required for the oxygen reduction

14

and the D-channel transports both protons for oxygen reduction and all the pumped protons [5-8]. Both channels take up protons from the N-side, but some of the protons taken up from the D-channel are transported to a currently unidentified proton exit site at the P-side. In cytochrome bo_3, unlike the cytochrome c oxidases, protons released from the ubiquinol oxidation reaction are also released to the P-side. To differentiate between the two proton releasing reactions (i.e., the pumped protons and protons released by ubiquinol oxidation) we again resorted to the E286C mutant, which does not pump but still releases protons from ubiquinol oxidation to the P-side. Fig.5 (bottom right) indicates that while proton uptake from the N-side is qualitative similar to WT cytochrome bo_3, the pH dependency on proton release at the P-side is not detected in the mutant. We therefore propose that the pH-dependency of proton transport activity by WT cytochrome bo_3 is due to proton release at the proton-exit site.
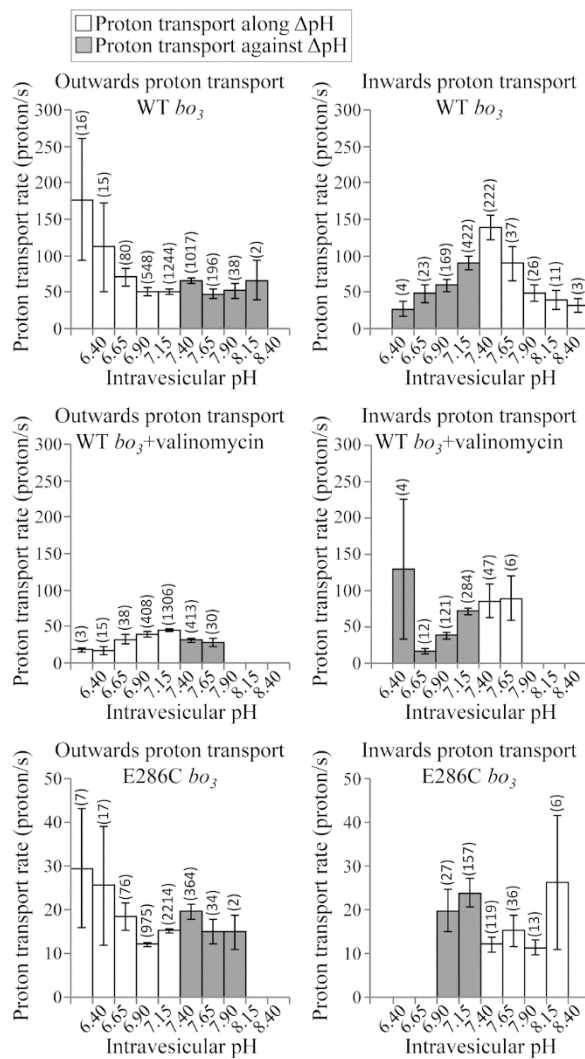
Fig. 5. The effect of intravesicular pH on the rate of proton translation in cytochrome bo_3. The top two subfigures show data from WT cytochrome bo_3; the middle are for WT cytochrome bo_3 with valinomycin; and the bottom two are for the E286C mutant. The three panels on the left correspond to cytochrome bo_3 transporting protons outwards (the alkalization of the lumen pH), while the three panels on the right correspond to transporting protons inwards (the acidification of the lumen pH). Shaded bars show cytochrome bo_3 transporting protons against the ΔpH, and the clear bars show the proton transportation along the ΔpH. Error bars represent the standard error of the mean. The value in brackets above each data point indicates the number of proteoliposomes containing a single cytochrome bo_3 observed under these conditions (n).

16

Conclusions

Using single-enzyme data, three enzyme properties of a HCO, cytochrome bo_3, were established. The proton transport rate is insensitive to pH between pH 6.4-8.4 on the *N*-side of the enzyme, while on the *P*-side the activity is optimal at a pH of about 7.4. Second, the proton transport rate is positively correlated to the size of the proteoliposome, i.e., the enzyme activity is negatively affected by membrane curvature. Finally, cytochrome bo_3 can enter a leak state either during turn-over or upon halting turn-over. While this suggests one of the intermediate oxidative states may be linked to leakage the mechanism by which cytochrome bo_3 leaks protons is currently unknown and is subject to further studies.

Materials and methods

Protein purification and reconstitution

All chemicals were purchased from Sigma-Aldrich unless otherwise stated. Wild-type and E286C cytochrome bo_3 were purified from *Escherichia coli* C43 strains with the bo_3 gene knocked out from chromosome, where proteins were expressed from pET plasmids containing the corresponding gene sequences [21]. Wild-type cytochrome bo_3 was also purified from GO105/pJRhisA [23] for comparison. Proteins were purified[39] and reconstituted[40] similarly as previously reported.

Cells expressing cytochrome bo_3 (typically in batches of 4 L culture) were resuspended after centrifugation (7000 g for 10 min) in W1 buffer (20 mM MOPS, 5 mM $MgSO_4$, 30 mM Na_2SO_4, pH 7.4) at 0.25 g cells/mL and were lysed by two passages through a cell disrupter (Constant Systems) at 35 kpsi. The lysed cells were centrifuges at 11000 g for 10 min to remove debris. The supernatant was further centrifuged at 100000 g for 1 h at 4 °C to harvest the cell membranes, which were resuspended in W1 buffer. After determining the protein concentration with a bicinchoninic acid (BCA) assay, the membranes were diluted to 3-4 mg/mL protein in solubilization buffer (20 mM tris/HCl, 5 mM $MgSO_4$, 300 mM NaCl, 20 mM imidazole, 10% glycerol and 1% n-dodecyl-β-maltoside (DDM, Anatrace), pH 8.0) and incubated 1 h at 4 °C. The mixture was again centrifuged at 100000 g for 45 min to remove insoluble material, after which the supernatant was loaded on a Ni-sepharose column (GE Healthcare, 2 mL Sepharose 6 Fast Flow) that was pre-equilibrated with equilibration buffer (20 mM tris/HCl, 5 mM $MgCl_2$, 10% Glycerol, 250 mM NaCl, 20 mM imidazole, 0.05 % DDM). The column was washed with at least 20 mL equilibration buffer A and then 20 mL

17

wash buffer B (same as equilibration buffer A, but with 40 mM imidazole). The protein was then eluded using a linear gradient in which the imidazole was increased to 200 mM. The protein was concentrated, and the buffer was exchanged for 20 mM MOPS, 30 mM NaSO$_4$, pH 7.4 in a 100 kDa MW cut-off ultrafiltration column (Vivaspin, Generon). After the protein concentration was determined with a BCA assay and using the adsorption of the Soret band at 408 nm, aliquots were stored at -80 °C at a concentration between 20 – 40 µM after snap freezing in liquid nitrogen.

Cytochrome *bo*$_3$ was reconstituted in *E. coli* polar lipids (Avanti Lipids). 5 mg of *E. coli* polar lipid was dissolved in 95 µL chloroform to which 50 µL 1 mg/mL ubiquinone-10 (in chloroform) and 20 µL (1 mg/mL) ATTO633-DOPE (ATTO-TEC GmbH, Germany) in chloroform was added. After the mixture was dried under vacuum for at least 1 h, it was hydrated in 0.5 mL of 20 mM MOPS, 30 mM NaSO$_4$, 5 mM 8-hydroxypyrene-1, 3, 6-trisulfonic acid trisodium salt (HPTS) and 55 mM octyl-β-D-glucopyranosde (OG). After the lipids were dissolved in this detergent solution, cytochrome *bo*$_3$ was added at a low protein-to-lipid ratio (0.073% w/w) and incubated on ice for 15 min. The mixture was then incubated sequentially in 0.05, 0.1 and 0.1 g of SM-2 Biobeads on ice for 1 h, 1h and 2h, respectively. After diluting the mixture (without the biobeads) with 20 mM MOPS, 30 mM NaSO$_4$, pH 7.4 to about 25 mL, the mixture was centrifuged at 100000 g for 1 h at 4 °C and the proteoliposome pellet was resuspended in 0.5 mL of the same buffer. Finally, the proteoliposomes solution was centrifuges at 17000 g for 5 min to remove debris and the supernatant was stored at 4 °C and used within 48 h for the single-enzyme electrochemistry-fluorescent experiments.

For the ensemble experiments, the same reconstitution protocol was used but at a higher protein-to-lipid ratio of 1% (w/w). After reconstitution, the proteoliposomes were treated with 10 freeze-thaw cycles to increase the average size of the vesicles. The size of the vesicles was measured with DLS as previously described [41]. The decylubiquinol oxidation activity was measured after which the liposome size of the same preparation was reduced by extruding them through 100 nm track-etched membranes and the activity measurement was repeated. The enzymatic activity assay was similar to that outlined in Rumbley *et al*. [39]. First the substrate, decylubiquinone (Sigma-Aldrich), was solubilized in absolute ethanol. The concentration of the prepared decylubiquinone solution was confirmed spectroscopically at 275 nm (ε = 19 mM^{-1}cm^{-1} in absolute ethanol). Decylubiquinone (DQ) was reduced to decylubiquinol using sodium borohydride crystals in a method similar to that described in

Trounce *et al*. [42]. To remove excess hydride ions remaining in the solution, 0.1 M HCl was added (1 µL per 10 µL of DUQ solution). For the assay, 70 µL of prepared proteoliposomes (5 mg/mL lipid), and 20 µL of 1.695 mM reduced DQ was diluted in HEPES buffer (40 mM HEPES, 20 mM NaCl, pH 7.4) to a final volume of 1 mL and the oxidation of DQ was monitored at 275 nm (ε = 12.25 mM^{-1}cm^{-1} in aqueous solution) for 5 min. The activity of cytochrome bo_3 is calculated by converting the absorbance reading at 275 nm into µmoles of DQ (using ε = 12250 M^{-1} cm^{-1}; [43]) and plotted against time. The initial slope of the curve in a plot of µmoles of DQ against time (gradient of the initial 20 seconds) is calculated and converted to represent rate of DQ turnover per cytochrome bo_3, where we used the previously determined reconstitution yield of ~50% [16, 44] (i.e., final protein-to-lipid ratio is ~0.5% (w/w; ~25 µg/mL in the proteoliposome solution) and a molecular weight of cytochrome bo_3 of 144 kDa (i.e. ~0.17 µM in the proteoliposome solution).

Electrochemistry-microscopy measurement

The experimental set-up was described in detail elsewhere [16]. Proteoliposomes/liposomes were sparsely absorbed to a highly smooth gold electrode functionalized by 6-mercapto-1-hexanol. Images and time-resolved image series were recorded using an inverted epi-fluorescence microscope (Nikon Instruments, U.K.). The frame rate is 2.6s. Typical image series contain about 500-1000 lipid vesicles. The ubiquinone pool in the vesicles' lipid bilayer can be electrochemically reduced (-0.2V vs. Standard Hydrogen Electrode) and initiates oxygen reduction and proton uptake/release in cytochrome bo_3. The recording of images starts without an electrochemical potential (pre-potential phase) followed by a 100s-phase (within-potential phase) with the electrochemical potential applied to the gold electrode (cytochrome bo_3 can transport protons in this phase). The potentiostat was then switched off again but the image recording would continue for certain amount of time (post-active phase). The total time span for each recording session is 300s. When the electrochemical potential is terminated, the proton uptake/release activity is found to halt within the time resolution of this study and, thus, the enzyme activity is tightly controlled by the potentiostat. There is a minimum of 15-minutes waiting period between each recording to allow the ΔpH and membrane potential to dissipate, and the fields of view of different recording sessions do not overlap. Typically, 5 recordings were done on each gold electrode. Each experimental system (wild-type bo_3, E286C mutant and valinomycin) contains data collected from different batches of purified proteins and with each protein batch, recordings with multiple electrodes were made. The number of independent lipid vesicles in

the experiment with the wild-type enzyme was about 69,000, of which about 4000 vesicles exhibit proton uptake/release. When required, valinomycin was added to a final concentration of 10 µM as described in detail elsewhere [16].

Data Analysis

The data analysis procedure is written in MATLAB language and was described in detail previously [16]. Before the start of an experiment a single fluorescence image was taken to obtain the ATTO-633 fluorescence intensity of individual proteoliposomes/liposomes, which was used to calculate the radius (r) of the individual proteoliposomes/liposomes. Time-resolved imaging data were recorded for HPTS fluorescence. Image series were registered and corrected for drifting using ImageJ StackReg plug-in [45]. All subsequent analysis was performed in MATLAB R2015a (MathWorks, Massachusetts, U.S.A.) using user-written code. Lipid vesicles were identified on each frame of the image series and a two-dimensional Gaussian function was used to fit each vesicle' HPTS fluorescence images. The ratio of the fluorescence intensity of HPTS with the two excitation filters was used to calculate the pH inside the individual proteoliposome/liposomes at the time of measurement, according to:

$$pH = pK_{app} + \log\left(\frac{R - R_a}{R_b - R}\right)$$

where R is the measured intensity ratio using the two excitation filters, pK_{app} is the apparent pK_a value of HPTS and R_a and R_b are the fluorescence intensity ratios of the protonated and unprotonated forms of HPTS, respectively.

The cumulative number of protons taken/released (ΔH^+_{total}) was then calculated based on the diameter of lipid vesicle, the pH change of a vesicle compared to the beginning of the recording (i.e., $(\Delta pH)_t = pH_t - pH_0$; where pH_t is the pH at time t and pH_0 the average pH of the pre-potential phase) and the buffering effect of MOPS buffer (ΔH^+_{MOPS}), HPTS (ΔH^+_{HPTS}) and the lipids (ΔH^+_{lipids}), according to:

$$\Delta H^+_{total} = \Delta H^+_{MOPS} + \Delta H^+_{HPTS} + \Delta H^+_{lipids}$$

In this definition, ΔH^+_{total} equals 0 at time=0. The concentrations of MOPS buffer and HPTS encapsulated within the lipid vesicles were assumed to be the same as the bulk solution. The buffering effect of MOPS and HPTS was calculated using a simple reordering of the Henderson-Hasselbach equation, taking into the account the internal volume (lumen) of the proteoliposomes (V) and the concentration of MOPS and HPTS (c_{MOPS} and c_{HPTS}). Positive

20

ΔH^+ is defined as protons being transported from the lumen of the vesicle to the outside bulk solution.

$$V = \frac{4}{3}\pi r^3$$

$$\Delta H^+_{MOPS} = N_A V \left(\frac{c_{MOPS}}{10^{\left(pH_0 - pK_{a_{MOPS}}\right)} + 1} - \frac{c_{MOPS}}{10^{\left(pH_t - pK_{a_{MOPS}}\right)} + 1} \right)$$

$$\Delta H^+_{HPTS} = N_A V \left(\frac{c_{HPTS}}{10^{\left(pH_0 - pK_{a_{HPTS}}\right)} + 1} - \frac{c_{HPTS}}{10^{\left(pH_t - pK_{a_{HPTS}}\right)} + 1} \right)$$

where pK_{a_MOPS} and pK_{a_HPTS} are the pK_as of MOPS and HPTS, respectively. N_A is the Avogadro constant.

The lipids are obtained from an *E. coli* extract and are a complex mixture of various lipids with different pK_as, where cardiolipin has been described to exhibit a complex protonation behavior around neutral pH [46]. Hence, the lipids' buffering capacity was determined empirically by a titration of liposomes between pH 3 and 11 beforehand and fitted to a 5th degree polynomial ($R^2 > 0.99$). To avoid overfitting, the smallest number of parameters was used without introducing obvious fitting errors. At the 4th degree, a fitting error over 8% was observed at pH=6 and hence a 5th degree polynomial was used. The buffer capacity was defined as ΔH^+ per lipid molecule as the function of pH (as determined from the pH titration). To do this, we estimated a weighted average of the lipid molecular weight and an average of the surface area per lipid molecule ($A_{lipid\ headgroup}$) [47]. Various alternative models were considered to fit the pH titration and describe the buffer capacity of the *E. coli* extract, but alternative models were not found to significantly change the determination of ΔH^+_{total}. The lipid surface area of the individual single vesicles was estimated from the vesicle size, according to:

$$A = 4\pi r^2$$

$$N = A / A_{lipid\ headgroup}$$

$$\Delta H^+_{lipids} = N \left(\left(apH_t^5 + bpH_t^4 + cpH_t^3 + dpH_t^2 + epH_t \right) \right.$$

$$\left. - \left(apH_0^5 + bpH_0^4 + cpH_0^3 + dpH_0^2 + epH_0 \right) \right)$$

where N is the number of lipid molecules in a vesicle, which is calculated from the vesicle surface area (A) and $A_{lipid\ headgroup}$. *a, b, c, d* and *e* are the parameters of the polynomial function that are obtained by fitting the results of the titration of a liposome solution (see above).

21

The sections of time traces recorded after the applied potential was switched off were fitted with an exponential decay function, where it was assume the pH would return to the pH in the lumen before the experiment started (i.e. pre-activity pH). We also analyzed the data assuming the pH would return the bulk pH (7.4) and, qualitatively, this produced the same results.

The sections of the time traces within the potential window were then analyzed using user-written code to detect the proton taken up/released and leaking events. This automatic analysis is based on the hypothesis that a correlation between the pH/number-of proton taken up/released and time indicates either an active proton uptake/release or leaking event. It consists of fitting the data to models of one or multiple joint lines and, for each line (segment), the calculation of Kendall tau rank correlation coefficient. In order to prevent over-fitting of the trace by multiple lines, the fitting would start with a single linear regression (a single segment). If the standard deviation of the residual was less than 110% of the standard deviation of the trace, the procedure was stopped and the Kendall tau value determined. The standard deviation of the trace is independently determined using the data prior to the application of the potential. It is assumed that the intravesicular pH before the applying a potential is constant and that the noise level is consistent during the entire trace. If the standard deviation of the residual of the segment is higher than 110%, the data is fitted to two joined segments (i.e., the start of the second segment joins with the end of the first segment), where an iterative process is used to determine, based on the best fit, at which time-point the two segments are connected. If any of the segments still has a residual with a standard deviation above 110%, this process is continued. To further check if the use of multiple segments is statistically justified, adjusted R^2 values are determined for fits using one, two or more segments, and the fit with the highest adjusted R^2 value is used. Adjusted R^2 is a suitable indictor because it takes into account the increase of the number of the variables in a fit. P-values were calculated as part of the Kendall test on the resolved sections from the model fitting and only the sections of time traces with P-values below the threshold of 0.05 (95% confidence level) were accepted as proton uptake/release or leaking events. Proton uptake/release or leaking rates are taken from the slopes of the segments. The data was analyzed with higher and lower confidence levels and was found to be qualitatively identical. Finally, a leak event is defined as a change in the sign of a slope for two adjoining segments, where it is assumed that the first segment is due to active proton uptake/release.

Supplementary information

Time-resolved fluorescence microscopic data (traces) of individual lipid vesicles with proton transport activity by single WT cytochrome bo_3, measured during this research, are openly available from the University of Leeds data repository at http://doi.org/10.5518/151. The MATLAB code for the analysis of proton transport activity in single liposomes is also openly available from the University of Leeds at http://doi.org/10.5518/150

References

[1] J. Abramson, S. Riistama, G. Larsson, A. Jasaitis, M. Svensson-Ek, L. Laakkonen, A. Puustinen, S. Iwata, M. Wikstrom, The structure of the ubiquinol oxidase from *Escherichia coli* and its ubiquinone binding site, Nat. Struct. Biol., 7 (2000) 910-917.

[2] A. Puustinen, M. Finel, M. Virkki, M. Wikstrom, Cytochrome *o* (*bo*) is a proton pump in *Paracoccus denitrificans* and *Escherichia coli*, Febs Lett, 249 (1989) 163-167.

[3] M.M. Pereira, M. Santana, M. Teixeira, A novel scenario for the evolution of haem-copper oxygen reductases, BBA-Bioenergetics, 1505 (2001) 185-208.

[4] S. Iwata, C. Ostermeier, B. Ludwig, H. Michel, Structure at 2.8-Ångstrom resolution of cytochrome *c* oxidase from *Paracoccus denitrificans*, Nature, 376 (1995) 660-669.

[5] P. Brzezinski, P. Adelroth, Design principles of proton-pumping haem-copper oxidases, Curr. Opin. Struc. Biol., 16 (2006) 465-472.

[6] V.R.I. Kaila, M.I. Verkhovsky, M. Wikstrom, Proton-coupled electron transfer in cytochrome oxidase, Chem. Rev., 110 (2010) 7062-7081.

[7] P.R. Rich, A. Marechal, Functions of the hydrophilic channels in protonmotive cytochrome *c* oxidase, J. R. Soc. Interface, 10 (2013).

[8] S. Yoshikawa, A. Shimada, Reaction mechanism of cytochrome *c* oxidase, Chem. Rev., 115 (2015) 1936-1989.

[9] K. Hirata, K. Shinzawa-Itoh, N. Yano, S. Takemura, K. Kato, M. Hatanaka, K. Muramoto, T. Kawahara, T. Tsukihara, E. Yamashita, K. Tono, G. Ueno, T. Hikima, H. Murakami, Y. Inubushi, M. Yabashi, T. Ishikawa, M. Yamamoto, T. Ogura, H. Sugimoto, J.R. Shen, S. Yoshikawa, H. Ago, Determination of damage-free crystal structure of an X-ray-sensitive protein using an XFEL, Nat. Methods, 11 (2014) 734-736.

[10] S.A. Siletsky, A.A. Konstantinov, Cytochrome *c* oxidase: Charge translocation coupled to single-electron partial steps of the catalytic cycle, BBA-Bioenergetics, 1817 (2012) 476-488.

[11] T. Ogura, Resonance Raman applications in investigations of cytochrome *c* oxidase, BBA-Bioenergetics, 1817 (2012) 575-578.

[12] Y.C. Kim, G. Hummer, Proton-pumping mechanism of cytochrome *c* oxidase: A kinetic master-equation approach, BBA-Bioenergetics, 1817 (2012) 526-536.

[13] D.M. Popovic, A.A. Stuchebrukhov, Coupled electron and proton transfer reactions during the O -> E transition in bovine cytochrome *c* oxidase, BBA-Bioenergetics, 1817 (2012) 506-517.

[14] M.R.A. Blomberg, P.E.M. Siegbahn, The mechanism for proton pumping in cytochrome *c* oxidase from an electrostatic and quantum chemical perspective, BBA-Bioenergetics, 1817 (2012) 495-505.

[15] S. Ferguson-Miller, C. Hiser, J. Liu, Gating and regulation of the cytochrome *c* oxidase proton pump, BBA-Bioenergetics, 1817 (2012) 489-494.

[16] M. Li, S.K. Jorgensen, D.G.G. McMillan, L. Krzemniski, N.N. Daskalakis, R.H. Partanen, M. Tutkus, R. Tuma, D. Stamou, N.S. Hatzakis, L.J.C. Jeuken, Single enzyme experiments reveal a long-lifetime proton leak state in a heme-copper oxidase, J. Am. Chem. Soc., 137 (2015) 16055-16063.

[17] I. Belevich, M.I. Verkhovsky, M. Wikstrom, Proton-coupled electron transfer drives the proton pump of cytochrome *c* oxidase, Nature, 440 (2006) 829-832.

[18] K. Faxen, G. Gilderson, P. Adelroth, P. Brzezinski, A mechanistic principle for proton pumping by cytochrome *c* oxidase, Nature, 437 (2005) 286-289.

[19] V.R.I. Kaila, V. Sharma, M. Wikstrom, The identity of the transient proton loading site of the proton-pumping mechanism of cytochrome *c* oxidase, BBA-Bioenergetics, 1807 (2011) 80-84.

[20] K. Faxen, P. Brzezinski, The inside pH determines rates of electron and proton transfer in vesicle-reconstituted cytochrome *c* oxidase, BBA-Bioenergetics, 1767 (2007) 381-386.

[21] T. Egawa, K. Ganesan, M.T. Lin, M.A. Yu, J.P. Hosler, S.R. Yeh, D.L. Rousseau, R.B. Gennis, Differential effects of glutamate-286 mutations in the aa_3-type cytochrome *c* oxidase from Rhodobacter sphaeroides and the cytochrome bo_3 ubiquinol oxidase from *Escherichia coli*, BBA-Bioenergetics, 1807 (2011) 1342-1348.

[22] S. Veshaguri, S.M. Christensen, G.C. Kemmer, G. Ghale, M.P. Moller, C. Lohr, A.L. Christensen, B.H. Justesen, I.L. Jorgensen, J. Schiller, N.S. Hatzakis, M. Grabe, T.G. Pomorski, D. Stamou, Direct observation of proton pumping by a eukaryotic P-type ATPase, Science, 351 (2016) 1469-1473.

[23] N.N. Daskalakis, A. Muller, S.D. Evans, L.J.C. Jeuken, Driving bioenergetic processes with electrodes, Soft Matter, 7 (2011) 49-52.

[24] H.T. McMahon, J.L. Gallop, Membrane curvature and mechanisms of dynamic cell membrane remodelling, Nature, 438 (2005) 590-596.

[25] J.B. Larsen, M.B. Jensen, V.K. Bhatia, S.L. Pedersen, T. Bjornholm, L. Iversen, M.J. Uline, I. Szleifer, K.J. Jensen, N.S. Hatzakis, D. Stamou, Membrane curvature enables N-Ras lipid anchor sorting to liquid-ordered membrane phases, Nat. Chem. Biol., 11 (2015) 192-194.

[26] K.M. Davies, C. Anselmi, I. Wittig, J.D. Faraldo-Gomez, W. Kuhlbrandt, Structure of the yeast F_1F_0-ATP synthase dimer and its role in shaping the mitochondrial cristae, P. Natl. Acad. Sci. U.S.A., 109 (2012) 13602-13607.

[27] N.S. Hatzakis, V.K. Bhatia, J. Larsen, K.L. Madsen, P.-Y. Bolinger, A.H. Kunding, J. Castillo, U. Gether, P. Hedegard, D. Stamou, How curved membranes recruit amphipathic helices and protein anchoring motifs, Nat Chem Biol, 5 (2009) 835-841.

[28] A. Tonnesen, S.M. Christensen, V. Tkach, D. Stamou, Geometrical membrane curvature as an allosteric regulator of membrane protein structure and function, Biophys. J., 106 (2014) 201-209.

[29] A.V. Botelho, T. Huber, T.P. Sakmar, M.F. Brown, Curvature and hydrophobic forces drive oligomerization and modulate activity of rhodopsin in membranes, Biophys. J., 91 (2006) 4464-4477.

[30] R.M. Epand, K. D'Souza, B. Berno, M. Schlame, Membrane curvature modulation of protein activity determined by NMR, BBA-Biomembranes, 1848 (2015) 220-228.

[31] K.R. Rosholm, N. Leijnse, A. Mantsiou, V. Tkach, S.L. Pedersen, V.F. Wirth, L.B. Oddershede, K.J. Jensen, K.L. Martinez, N.S. Hatzakis, P.M. Bendix, A. Callan-Jones, D. Stamou, Membrane curvature regulates ligand-specific membrane sorting of GPCRs in living cells, Nat Chem Biol, (2017).

[32] M.L. Verkhovskaya, A. GarciaHorsman, A. Puustinen, J.L. Rigaud, J.E. Morgan, M.I. Verkhovsky, M. Wikstrom, Glutamic acid 286 in subunit I of cytochrome bo_3 is involved in proton translocation, P. Natl. Acad. Sci. U.S.A., 94 (1997) 10128-10131.

[33] P. Nicholls, J. He, Direct and indirect effects of valinomycin upon cytochrome *c* oxidase, Arch. Biochem. Biophys., 301 (1993) 305-310.

[34] C.L. Kuyper, J.S. Kuo, S.A. Mutch, D.T. Chiu, Proton permeation into single vesicles occurs via a sequential two-step mechanism and is heterogeneous, J. Am. Chem. Soc., 128 (2006) 3233-3240.

[35] D.A. Bloch, A. Jasaitis, M.I. Verkhovsky, Elevated proton leak of the intermediate O_H in cytochrome *c* oxidase, Biophys. J., 96 (2009) 4733-4742.

[36] J. Berg, S. Block, F. Höök, P. Brzezinski, Single proteoliposomes with *E. coli* quinol oxidase: Proton pumping without transmembrane leaks, Isr. J. Chem., 57 (2017) 437-445.

[37] H. Felle, J.S. Porter, C.L. Slayman, H.R. Kaback, Quantitative measurements of membrane potential in *Escherichia coli*, Biochemistry-Us, 19 (1980) 3585-3590.

[38] M.R.A. Blomberg, P.E.M. Siegbahn, Proton pumping in cytochrome *c* oxidase: Energetic requirements and the role of two proton channels, BBA-Bioenergetics, 1837 (2014) 1165-1177.

[39] J.N. Rumbley, E.F. Nickels, R.B. Gennis, One-step purification of histidine-tagged cytochrome *bo*$_3$ from *Escherichia coli* and demonstration that associated quinone is not required for the structural integrity of the oxidase, Biochim. Biophys. Acta-Protein Struct. Molec. Enzym., 1340 (1997) 131-142.

[40] M.L. Verkhovskaya, A. GarciaHorsman, A. Puustinen, J.L. Rigaud, J.E. Morgan, M.I. Verkhovsky, M. Wikstrom, Glutamic acid 286 in subunit I of cytochrome bo(3) is involved in proton translocation, Proc. Natl. Acad. Sci. U. S. A., 94 (1997) 10128-10131.

[41] S. Khan, M.Q. Li, S.P. Muench, L.J.C. Jeuken, P.A. Beales, Durable proteo-hybrid vesicles for the extended functional lifetime of membrane proteins in bionanotechnology, Chem Commun, 52 (2016) 11020-11023.

[42] I.A. Trounce, Y.L. Kim, A.S. Jun, D.C. Wallace, Assessment of mitochondrial oxidative phosphorylation in patient muscle biopsies, lymphoblasts, and transmitochondrial cell lines, Methods Enzymol, 264 (1996) 484-509.

[43] F.L. Crane, R. Barr, Determination of ubiquinones, in: Methods in Enzymology, Academic Press, 1971, pp. 137-165.

[44] L.J.C. Jeuken, S.D. Connell, P.J.F. Henderson, R.B. Gennis, S.D. Evans, R.J. Bushby, Redox enzymes in tethered membranes, J. Am. Chem. Soc., 128 (2006) 1711-1716.

[45] P. Thevenaz, U.E. Ruttimann, M. Unser, A pyramid approach to subpixel registration based on intensity, IEEE T. Image Process., 7 (1998) 27-41.

[46] P. Nollert, H. Kiefer, F. Jahnig, Lipid vesicle adsorption versus formation of planar bilayers on solid surfaces, Biophys. J., 69 (1995) 1447-1455.

[47] K. Murzyn, T. Rog, M. Pasenkiewicz-Gierula, Phosphatidylethanolamine-phosphatidylglycerol bilayer as a model of the inner bacterial membrane, Biophys. J., 88 (2005) 1091-1103.
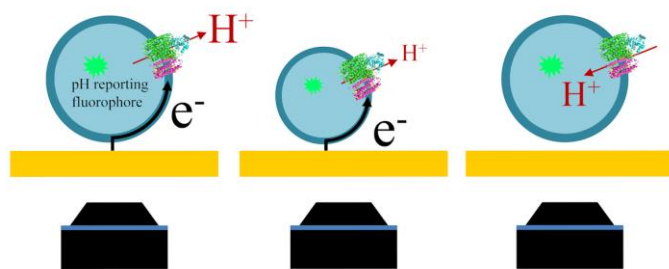
Graphical abstract

28

Highlights
- Proton transport measurements of single heme-copper oxidases
- Activity decreases with curvature of the lipid membrane
- Activity dependent on pH on the P-side, but not the N-side of the protein
- Contribution to proton leakage after turn-over has been halted